Heat transfer measurements on a circular cylinder in hypersonic flow

G. Park, S. L. Gai, A. J. Neely

School of Aerospace, Civil, and Mechanical Engineering
UNSW@ADFA, Canberra, ACT 2600, Australia

Abstract

The present paper discusses the experimental approach and results of surface heat flux on a circular cylinder at hypersonic speeds. The experiments were conducted using a free piston shock tunnel at a nominal Mach number of 10 with total enthalpies of 3.98MJ/kg and 13.5MJ/kg. The two-dimensionality of flow over the forebody as well as the base region was investigated. The forebody heat transfer results at the low enthalpy condition agreed well with the theories of Lees as well as Kemp, Rose, and Detra which assume equilibrium flow. At the high enthalpy condition, the heat transfer was dominated by both diffusion and conduction in the front stagnation region. The base region heat transfer data showed a local minimum at around $130°$ and $140°$ from the front stagnation point for low and high enthalpy conditions, respectively. This was followed by a gradual recovery towards the rear stagnation region. It was observed that the angles of heat transfer minima nearly coincide with the angles of flow separation.

Introduction

In designing spacecraft and re-entry type capsules, an accurate prediction of surface heat flux is very important since it determines the weight of thermal protection systems.

The forebody heat flux of various re-entry type capsules can readily be predicted by applying the existing theories ([1], [2]) or using available experimental data (for example, [3], [4], and [5]).

In contrast, the prediction of base region heating is quite challenging. One reason is the lack of experimental data that is available. Second, the flow in the base region is one of the most challenging areas that is not easily amenable to theoretical analysis. This is due to the fact that many complicated phenomena occur simultaneously such as the interaction of the lip shock and the shear layer, the interaction of the shear layer with the recirculation vortex, and also the possibility of supersonic reverse flow as predicted by Gnoffo in his CFD calculations [6]. Moreover, the heating rates in the base region are also influenced by the entropy layers resulting from a strong bow shock in the forebody region.

As a first step, therefore, the present paper discusses some experimental results of surface heat flux on a circular cylinder at hypersonic hypervelocity where the flow conditions are comparable to those of re-entry type capsules.

The experiments were conducted using a free piston shock tunnel and the surface heat flux on the forebody as well as the base region were measured using surface thermocouples. It must be pointed out that while there is some available data on pressures in the base region of a circular cylinder in hypersonic flow (for example, Dewey [7], McCarthy and Kubota [8], and Token and Oguro [9]), comparable data for base region heat flux does not exist.

The results of the forebody heat flux will be discussed and compared to the theories of Lees [1] as well as Kemp et al. [2] which are based on local similarity with the assumption of thermodynamic equilibrium in the boundary layer. Using Lees theory [1], the two limiting cases of heat transfer will be investigated and compared to the present experimental data.

The first limiting case is based on thermodynamic equilibrium in the boundary layer where the heat transfer is purely due to thermal conduction. The second limiting case considers diffusion rate controlled heat transfer under the assumption of very slow recombination rates within the boundary layer and fully catalytic surface.

The heat transfer in the base region will be discussed and compared to the supersonic flow data of Tewfik and Giedt [10]. Moreover, the features of flow separation will be discussed and compared to the available data.

The motivation to conduct these experiments using a circular cylinder is due to the fact that it is a generic blunt geometry on which a large body of information exists especially at subsonic and supersonic speeds. Secondly, it is a simple configuration with which to study such basic properties as surface heat flux and flow separation at high Mach numbers. An extension of the experiments to axisymmetric configurations such as Mars microprobe are planned and preparation of the model is currently underway.

Experiments

Model and instrumentation

The experiments were conducted using the free piston shock tunnel T-ADFA located in the School of Aerospace, Civil, and Mechanical Engineering at UNSW@ADFA in Canberra.

The model used in the present study was a circular cylinder with an outer diameter of 32mm and a span of 132mm. It was supported by side struts with chamfered end plates on both sides to minimise end effects and to produce an acceptable two-dimensional flow.

Each thermocouple was located every $20°$ apart along the azimuth and several thermocouples were also located off center to check the two-dimensionality of the flow. Fig.1 shows a schematic of the model installation and thermocouple locations.
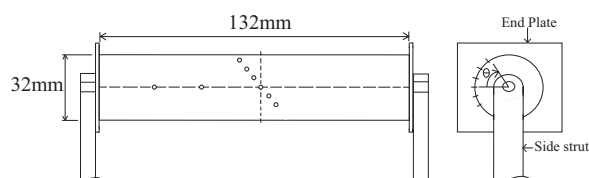

Figure 1: Thermocouple locations on the model

In the present experiments, K-type co-axial thermocouples were used to measure the surface heat flux. The reason for choosing K-type thermocouples was that they are quite robust and have fast signal response. With care, they can be manufactured to

have a rise time of approximately $1\mu s$ and a frequency response better than 100kHz [11].

The thermocouple consisted of a chromel wire fitted coaxially within a hollow cylinder of alumel. The outer diameter of each thermocouple was 2mm and its length was 3mm. Sand paper was used to form a junction resulting in tiny strands between the end of dissimilar metals. The sensitivity of a K-type thermocouple is $40\mu V/K$ at room temperature [12]. For the present study, this order of sensitivity was acceptable since the temperature change is relatively small (usually less than $25°$).

The heat flux is based on the time history of temperature which can be calculated using the relation [12]:

$$q_s(t_n) = \frac{\sqrt{\rho ck}}{\sqrt{\pi}} \sum_{i=1}^{n} \frac{T(t_i) - T(t_{i-1})}{(t_n - t_i)^{1/2} + (t_n - t_{i-1})^{1/2}} \quad (1)$$

where $\sqrt{\rho ck}$ is known as the thermal product of the substrate and $T(t_i)$ is the temperature as a function of time. The thermocouple signals are amplified using an amplifier which has an internal resistance of 99Ω producing a gain of 1000.

The thermocouples were calibrated using a water dipping technique [13] and the thermal product was determined to be 9690 ± 300 $Ws^{0.5}/m^2K$ throughout the calibration. The typical resistance of the thermocouples was approximately 1.4Ω.

Flow conditions

The present experiments were conducted using two flow conditions. The details of the nozzle reservoir and the free-stream conditions are presented in Table.1.

Conditions	A	B
h_o (MJ/kg)	13.5	3.98
p_o (MPa)	12	12
u_∞ (m/s)	4559	2513
T_∞ (K)	568	142
p_∞ (Pa)	359	251
ρ_∞ (kg/m^3)	0.002	0.0061
M_∞	9.37	10.9
Re_∞ (1/m)	3.26×10^5	1.47×10^6
N_2	0.69	0.76
O_2	0.081	0.19
N	0	0.00001
O	0.18	0.001
NO	0.044	0.045

Table 1: Flow conditions. Subscripts o and ∞ refer to the nozzle reservoir and the free-stream conditions, respectively. N_2, O_2, N, O, and NO are the mole fractions. Other symbols have their usual meanings.

The nozzle reservoir conditions were calculated using the computer program ESTC [14] which assumes chemical and vibrational equilibrium throughout. ESTC calculates the reservoir conditions by matching the reflected shock pressure to the measured reservoir pressure under the assumption of isentropic expansion. The nozzle exit conditions were calculated using STUBE [15] which is based on one-dimensional, chemically reacting inviscid nozzle flow.

A conical nozzle was used for the present study. It had $7.5°$ of divergence with an exit diameter of 300mm, and a throat diameter of 12.7mm. The effective core of the nozzle exit was found to be approximately 200mm. The high enthalpy condition consists of a reacting flow with 18% dissociated oxygen and no dissociation of nitrogen. The low enthalpy condition consists of non-reacting flow where a negligible amount of dissociation occurs. The test gas was air throughout.

Theoretical considerations

According to Lees [1], the surface heat flux can be calculated by using two limiting cases. The first uses an assumption of thermodynamic equilibrium where the surface heat flux purely comes from thermal conduction.

The expression used for this case is [1]:

$$q_{eq} = 0.47\sigma^{-2/3}\sqrt{(\rho_e\mu_e)_s}\sqrt{u_\infty}h_{se}F(S) \quad (2)$$

where

$$F(S) = \frac{(1/\sqrt{2})(P/P_s)(w/w_s)(u_e/u_\infty)r_o^k}{\sqrt{\int_o^s (P/P_s)(u_e/u_\infty)(w/w_s)r_o^{2k}ds}} \quad (3)$$

Here, $k=0$ for a two-dimensional body and $k=1$ for an axisymmetric body, w=ratio of viscosity over the product of universal gas constant and temperature, σ=Prandlt number, s=distance along the surface from the front stagnation point, r_0=body radius, h_{se}=enthalpy at front stagnation point, and s=conditions at front stagnation point.

The post-shock and front stagnation properties were calculated by using the computer program, EQSTATE, assuming equilibrium chemistry throughout [16].

The second limiting case, however, considers diffusion rate controlled heat transfer under the assumption of very slow recombination rates within the boundary layer and a fully catalytic surface.

The maximum difference in heat transfer between the two cases can be expressed as [1]:

$$\frac{q_{cond} + q_{diff}}{q_{eq}} \simeq \left\{ [1-A] + Le^{2/3}A \right\} \quad (4)$$

where

$$A = \frac{\sum h_{iw}(C_{ie} - C_{iw})}{h_{se}} \quad (5)$$

Here, Le=Lewis number, h_{iw}=enthalpy of ith species at the wall, C_{iw} and C_{ie}=concentration by weight of ith species at the wall and the edge of the boundary layer, respectively, and h_{se}=enthalpy at the front stagnation point

It should be noted that the actual surface heat flux is expected to lie in between these two limiting cases as long as the flow is regarded as continuum.

Besides Lees theory, the theoretical surface heat flux used in the present study is due to Kemp et al.[2]. This is an extension of the stagnation point theory of Fay and Riddell [17] where the surface heat flux is obtained using the concept of local similarity and variable external pressure gradient. Similar to the first limiting case of Lees theory, an equilibrium boundary layer is assumed throughout.

The expression used by Kemp et al.[2] is:

$$\frac{q}{q_s} = \left(\frac{r\rho_w\mu_w u_e}{\sqrt{2\xi}} \right) \left(2\rho_{ws}\mu_{ws}\left(\frac{du_e}{dx}\right)_s \right)^{-1/2} \left(\frac{g_{\eta w}}{g_{\eta ws}} \right) \quad (6)$$

where

$$\frac{[g_{\eta w}/(1-g_w)]}{[g_{\eta ws}/(1-g_{ws})]} = \frac{(1+0.096\sqrt{\beta})}{(1+0.096\sqrt{0.5})} = \frac{(1+0.096\sqrt{\beta})}{1.068} \quad (7)$$

and for a two-dimensional body

$$\xi = 0.5x^2 \rho_{ws}\mu_{ws}\left(\frac{du_e}{dx}\right)_s \quad (8)$$

Here, β=pressure gradient, η=distance normal to the surface, s=conditions at front stagnation point, r=body radius, $(du_e/dx)_s$=velocity gradient at stagnation point, ρ_w=density at the wall, μ_w=viscosity at the wall, u_e=velocity at the edge of boundary layer, and g_w=wall to the edge of boundary layer enthalpy ratio

When obtaining the surface heat flux using the theories of Lees and Kemp et al., the pressure distribution around the surface was calculated using the expression given by Tewfik and Giedt [10] for a circular cylinder. The heat transfer results of Tewfik and Giedt were obtained using their empirical expression [10]. In using equation (6), the stagnation point heat flux was calculated by Lees theory.

Results and discussion

The two dimensionality of flow

In obtaining accurate and reliable measurements of the surface heat flux on the circular cylinder model, it was essential to establish two-dimensionality of the flow. This was accomplished by using 8 thermocouples spanwise on the same azimuthal line which built up from multiple shots using the model described previously.

Fig.2 shows these results on the forebody as well as the base region. Here, q_{avg} is the averaged surface heat flux at the corresponding inclination. The errorbar denotes the typical shot-to-shot variation of heat transfer in the 95% confidence interval.

We note that the flow is reasonably two-dimensional both on the forebody as well as the base region. However, it should be pointed out that the variation of surface heat flux in the base region was relatively large, typically $\pm20\%$. One reason is that, in the base region, the temperature changes are quite small (typically less than $1°$) so that the signal to noise ratio becomes correspondingly small. The base region data of condition B were similar.

The forebody heat transfer

The typical heat transfer traces in the forebody region are shown in Fig.3. The thermocouple signals were filtered using the 3rd order polynomial Savitzky-Golay smoothing filters to remove high frequency noise. A Savitzky-Golay filter was chosen as it provides much smoother signals than the other standard averaging filters which tend to filter out a significant portion of the signal's high frequency content along with the noise.

In regard to Fig.3, there are steep gradients in heat transfer at the beginning of the flow for both conditions which are due to the shock arrival. The flow establishment process then takes place, lasting approximately $320\mu s$ for condition A and $820\mu s$ for condition B. After the flow establishment process, the steady flow lasts approximately $150\mu s$ for condition A and $500\mu s$ for condition B. The variation of the averaged heat flux in the forebody region at various azimuthal positions during the steady flow period was within $\pm7\%$ for both flow conditions. This indicates
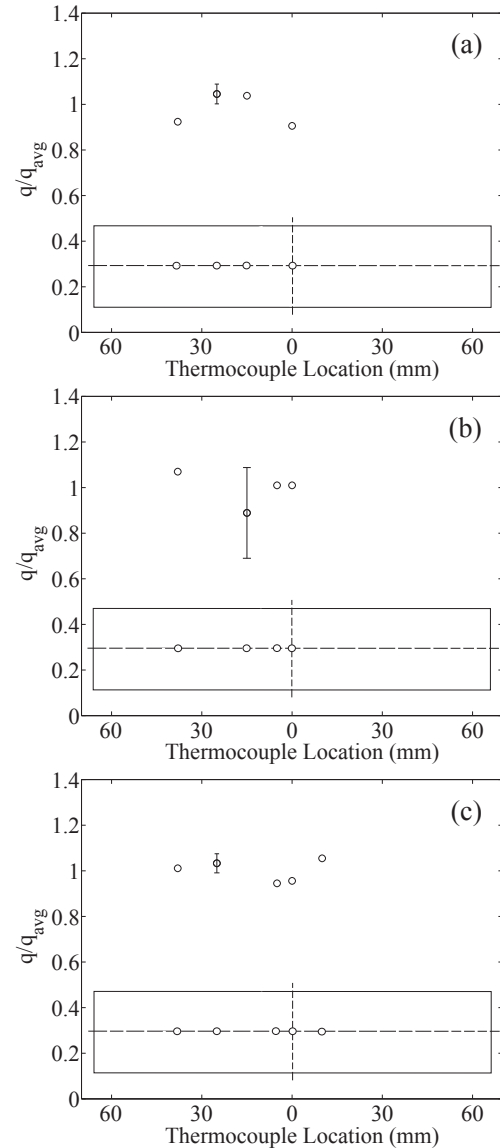

Figure 2: Two dimensionality of flow: (a) At the front stagnation point (Condition A) (b) 170° from the front stagnation point (Condition A) (c) At the front stagnation point (Condition B)

the flow is reasonably stable during the steady flow period at least for the surface heat flux.

The flow establishment can be characterised in terms of a non-dimensional parameter to make direct comparison against the existing data. It can be expressed as:

$$\tau_{est} = \frac{t_{est}u_\infty}{D} \quad (9)$$

where t_{est} is the time required to establish steady flow, D is a model diameter, and u_∞ is the free-stream velocity. In the present experiments, this parameter was found to be approximately 46 for condition A and 64 for condition B in the forebody region. The details regarding the flow establishment in the base region are discussed in the next section.

Fig.4 shows the comparison between the theory and the present experimental data in the forebody region. Note that the error
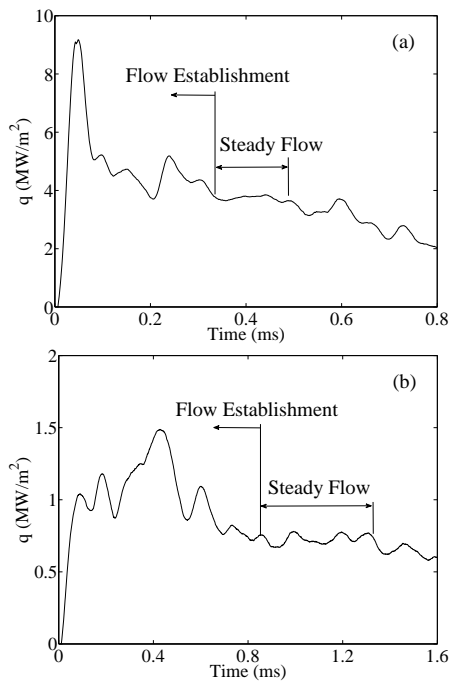
Figure 3: Typical traces of heat transfer in the forebody at $\theta=0°$. (a) Condition A (b) Condition B

bars denote the shot-to-shot variations of the averaged steady heat flux.

In regard to Fig.4.(a), it is seen that the heat flux in the front stagnation region lie close to the values where the heat flux are due to both diffusion and conduction. However, as the flow progresses around the surface, the heat transfer seems to lie closer to the limit of equilibrium where the heat transfer is purely conduction driven. This indicates that for condition A, the amount of heat transfer due to the recombination of dissociated species at the surface is quite significant in the front stagnation region.

From Fig.4(b), it can be seen that the experimental results lie close to the equilibrium limit where the heat transfer is purely due to conduction. Thus, in low enthalpy flow, the heat transfer due to chemical reactions at the surface is quite negligible since most of the dissociated species tend to get recombined in the gas phase and equilibrium is reached at the surface.

The base region heat transfer

The typical heat transfer traces of the base region for both flow conditions are presented in Fig.5. Again, the high frequency noise from the thermocouple signals was removed using the 3rd order polynomial Savitzky-Golay smoothing filters.

It is seen that the level of fluctuations of heat flux is quite comparable to the forebody signal traces. Secondly, the heat flux are substantially lower than the heat flux in the forebody region. This is bacause of the much lower density in the base region.

We also note that the steady flow is observed almost at the same time as for the forebody and the steady flow duration is also quite similar. When the flow establishment parameter of the base region is compared to the data of Holden [18], it is found to be similar.

Fig.6 shows the surface heat transfer distribution in the base region. It is seen that there is a distinct local minimum at about 140° and 130° from the front stagnation point for conditions
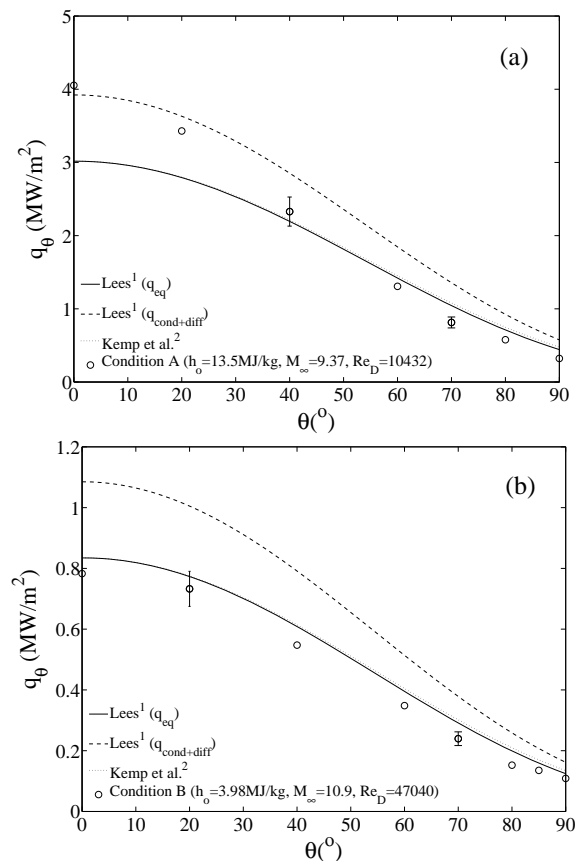

Figure 4: Heat transfer comparison in the forebody. (a) Condition A (b) Condition B

A and B, respectively. The distributions then show a gradual recovery towards the rear stagnation region for both flow conditions. This recovery in heat transfer is due to the momentum of the re-circulating flow.

We also note that the heat transfer ratios in the present experiments are consistently lower than the results of Tewfik and Giedt [10] in supersonic flow. This is thought to be the result of the lower density in the base region, a consequence of the high hypersonic free-stream Mach number.

The error bars in Fig.6 denote the shot-to-shot variations of the averaged steady heat flux. It is interesting to compare this data and what it tells us about flow separation with the pressure data behind a cylinder in hypersonic flow obtained by Dewey [7] as well as McCarthy and Kubota [8].

Flow separation

In the previous section, it was mentioned that there is a distinct local minimum in heat transfer at about 140° and 130° from the front stagnation point for conditions A and B, respectively.

It is believed that the angles delineating heat transfer minimum relate to the angles of flow separation. This can be confirmed by comparing the data of [19] where flow visualisation experiments were conducted using the same model and the same flow conditions.

Fig.7 shows the dependency of the separation angle on Reynolds number. The present data are compared with the available experimental data.

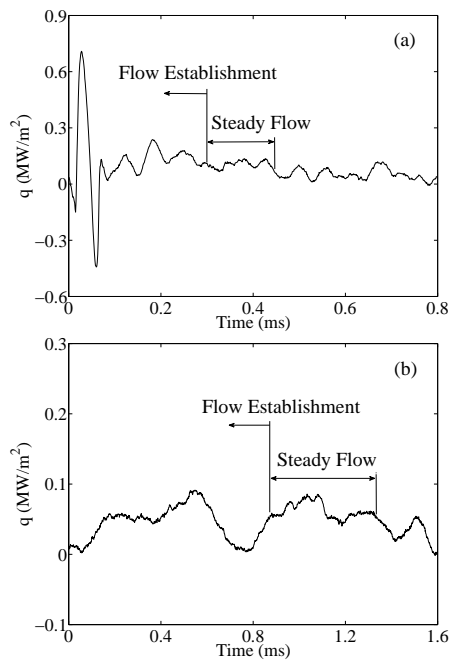Here, the Reynolds number is based on the free-stream condi-

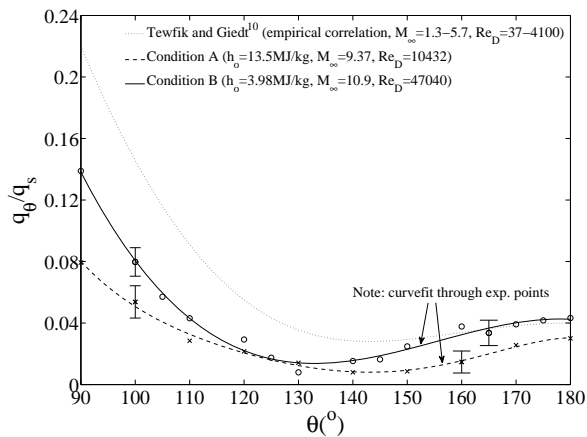Figure 5: Typical traces of heat transfer in the base at $\theta=180°$. (a) Condition A (b) Condition B

Figure 6: The base region heat transfer

Figure 7: The flow separation angle on a circular cylinder: Dewey [7], (1) $M_\infty=6$; McCarthy and Kubota [8], (2) $M_\infty=5.7$; Token and Oguro [9], (3) $M_\infty=14$; Tewfik and Giedt [10], (4) $M_\infty=1.32$ (5) $M_\infty=2.19$; Hruschka et al. [19], (6) $M_\infty=10$; Metcalf et al. [20], (7) $M_\infty=1.7$ (8) $M_\infty=2.12$; Gregorek and Korkan [21], (9) $M_\infty=10.6$ (10) $M_\infty=12.6$ (11) $M_\infty=15.37$; Gowen and Perkins [22], (12) $M_\infty=1.98$, (13) $M_\infty=1.49$ (14) $M_\infty=2.9$; Present data, (15) $M_\infty=10$

front stagnation region. As the flow progresses away from the front stagnation region, the heat transfer was close to the equilibrium limit.

The heat transfer distribution in the base region indicated that there is a local minimum at about 140° and 130° from the front stagnation point for conditions A and B, respectively. The distributions then showed a gradual recovery towards the rear stagnation region for both flow conditions.

It was found that the separation angle increased with a decrease in Reynolds number. It was also found that the flow separation angle nearly coincides with the angle of heat transfer minimum.

Acknowledgements

References

[1] Lester Lees, Laminar heat transfer over blunt-nosed bodies at hypersonic flight speeds, Jet Propulsion, Vol. 26, No.4, 1956, 259-269

[2] Nelson H. Kemp, Peter H. Rose and Ralph W. Detra, Laminar heat transfer around blunt bodies in dissociated air, Journal of the aerospace sciences, July, 1959, 421-430

[3] R. Bur, R. Benay, B. Chanetz, A. Galli, T. Pot, B. Hollis and J. Moss, Experimental and numerical study of the Mars Pathfinder vehicle, Aerospace Science and Technology 7, 2003, 510-516

[4] R. Hollis and J. N. Perkins, Transition effects on heating in the wake of a blunt body, AIAA-97-2569, AIAA Thermodynamics conference, 32nd, Atlanta, GA, June 23-25, 1997

[5] T. J. Horvath and Klaus Hannemann, Blunt body near-wake flow field at Mach 10, AIAA-1997-986, Aerospace Sciences Meeting and Exhibit, 35th, Reno, NV, Jan. 6-9, 1997

tions and the model diameter. It is seen that in the low to moderate Reynolds number range ($10^2 \leq Re_D \leq 10^6$), the separation angle varies between 145° and 120°.

It is seen that the separation angle decreases as Reynolds number increases. Note that the validity of experimental data for Reynolds numbers less than 100 becomes uncertain as at such low Reynolds numbers, the thin boundary layer assumption itself becomes questionable.

It is seen that the present data is in reasonably good agreement with other hypersonic cylinder data.

Conclusions

The experimental results of surface heat flux on a circular cylinder at hypersonic speeds are reported. The forebody heat transfer distribution agreed well with the theories of Lees as well as Kemp et al. for the low enthalpy flow, condition B.

In high enthalpy flow, condition A, a significant portion of the heat transfer was due both to diffusion and conduction in the
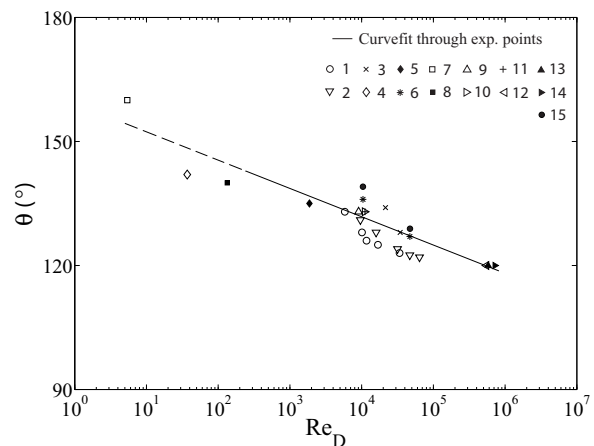
[6] Peter A. Gnoffo, Planetary-entry gas dynamics, Annu. Rev. Fluid. Mech., Vol.31, 1999, 459-494

[7] C. Forbes Dewey Jr., Near-wake of a blunt body at hypersonic speeds, AIAA journal, Vol.3, No.6, 1965, 1001-1010

[8] John F. McCarthy Jr. and Toshi Kubota, A study of wakes behind a circular cylinder at M=5.7, AIAA journal, Vol.2, No.4, 1964, 629-636

[9] K. H. Token and H. Oguro, Experimental investigations of hypersonic flow around two-dimensional circular cylinders, Aerospace Research Laboratories Rep., Oct, 1965, 65-212

[10] O. K. Tewfik and W. H. Giedt, Heat transfer, recovery factor, and pressure distributions around a circular cylinder normal to a supersonic rarefied-air stream, J. Aero. Sci., Vol.27, No.10, 1960, 721-729

[11] S. L. Gai and N. R. Mudford, Stagnation point heat flux in hypersonic high enthalpy flow, Shock Waves, 1992, 43-47

[12] Schultz, D. L. and Jones, T. V., Heat transfer measurements in short-duration hypersonic facilities, AGARDograph No 165., 1973

[13] S. G. Mallinson, Shock wave/boundary layer interaction at a compression corner in hyper-velocity flows, 1994, PhD Thesis, University of New South Wales

[14] McIntosh, M., A computer program for the numerical calculation of equilibrium and perfect gas conditions in shock tunnels, Tech. Rep. CPD 169, Australian Defence Scientific Service, 1968

[15] Vardavas, I. M., Modelling reactive gas flows within shock tunnels, Australian Journal of Physics, Vol.37, No.2, 1984, 157-177

[16] Rizkalla, O., EQSTATE: program to calculate the equilibrium or frozen properties of a supersonic gas flow at the static and stagnation points upstream and downstream of a shock wave, General Applied Science Laboratories Inc., New York., 1990

[17] J. A. Fay and F. R. Riddell, Theory of stagnation point heat transfer in dissociated air, J. Aeronautical Sciences, Vol.25, No.2, Feb, 1958, 73-85

[18] Michael, S. Holden, Establishment time of a laminar separated flows, AIAA journal, Vol.9, No.11, Nov, 1971, 2296-2298

[19] R. Hruschka, S. O'Byrne, H. Kleine, Near-resonantly-enhanced schlieren for wake flow visualisation in shock tunnels, 16th Australasian Fluid Mechanics Conference, Dec, 2007

[20] S. C. Metcalf, C. J. Berry, and Miss B. M. Davis, An investigation of the flow about circular cylinders placed normal to a low-density supersonic stream, A.R.C. Rep. and Memoranda, London, April, 1964, Rep. No.3416

[21] G. M. Gregorek and K. D. Korkan, An experimental observation of the Mach and Reynolds number independence of cylinders in hypersonic flow, AIAA journal, Vol.1, No.1, 210-211, 1963

[22] Forrest E. Gowen and Edward W. Perkins, Drag of circular cylinders for a wide range of Reynolds numbers and Mach numbers, NACA, TN-2960, June, 1953